Fast quantum gates for neutral atoms separated by a few tens of micrometers

Matteo Bergonzoni [1,*] Rosario Roberto Riso [1,2] and Guido Pupillo [1,†]
[1] *University of Strasbourg and CNRS, CESQ and ISIS (UMR 7006), Strasbourg 67000, France*
[2] *Department of Chemistry, Norwegian University of Science and Technology, Trondheim 7491, Norway*

(Received 30 November 2025; revised 6 February 2026; accepted 13 April 2026; published 15 September 2026)

We present a theoretical scheme for a family of fast and high-fidelity two-qubit ISWAP gates between neutral atoms separated by more than 20 μm, enabled by resonant dipole-dipole spin-exchange interactions between Rydberg states. The protocol harnesses coherent excitation-exchange-deexcitation dynamics between the qubit and the Rydberg states within a single and smooth laser pulse, in the presence of strong dipole-dipole interactions. We utilize optimal control methods to achieve theoretical gate fidelities and durations comparable to blockade-based gates in the presence of relevant noise, while extending the effective interaction range by an order of magnitude. This enables entanglement well beyond the blockade radius, offering a route toward fast, high-connectivity quantum processors.

DOI: 10.1103/hjrh-4327

I. INTRODUCTION

Neutral atoms trapped in optical tweezers are a leading platform for quantum computing, enabling low-defect arrays of thousands of atoms with arbitrary geometries, long qubit coherence times, and fast, high-fidelity two-qubit gates [1–6]. Most two-qubit gates rely on the Rydberg blockade, where van der Waals (vdW) interactions $V_{\mathrm{vdW}}(R) \sim R^{-6}$ between Rydberg-excited states suppress multiple excitations of nearby atoms [3–11], limiting the interaction range to a few micrometers. Alternative approaches such as the Rydberg antiblockade with vdW [12–14] or dipole-dipole $J(R) \sim R^{-3}$ [15] interactions have achieved similar ranges. Extending the entangling range without sacrificing speed or fidelity is, however, crucial for scalable, error-corrected architectures [2,16]. Experimentally, entangling atoms over tens of micrometers is achieved via qubit shuttling—moving the tweezers—on hundred-microsecond timescales [16–18]. Alternatively, DC or microwave fields can tune the Förster defect between selected Rydberg states enhancing the interaction strength, but such schemes are highly sensitive to field fluctuations and atomic positioning [19,20]. Another approach employs ancillary atoms to mediate interactions, at the cost of increased atomic overhead and longer gate times [21–23].

Here, we introduce a family of fast two-qubit gates based on resonant dipolar exchange interactions $J(R) \sim R^{-3}$ between atoms separated by tens of micrometers [15,24–30]. The protocol implements coherent excitation to, and deexcitation from, the Rydberg manifold—where rapid resonant exchange occurs—from long-lived ground-state qubits, enabling submicrosecond ISWAP gates (Fig. 1). While reminiscent of Rydberg antiblockade schemes [12–15], our approach introduces qualitatively new elements: a single global, continuous laser pulse with a *time-varying phase* optimized via quantum optimal control to realize gates that are *time-optimal* (TO) and *robust* against dominant error sources, including vdW interactions and spontaneous emission. The resulting fidelities and gate times are comparable to blockade-based protocols, while extending the interaction range by nearly an order of magnitude, enabling long-range entanglement in near-term quantum memories and processors. Similar schemes for ISWAP gates with Sr atoms have also been proposed in Ref. [31].

We consider two atoms, labeled $\alpha = A$ and B, separated by distance R [Fig. 1(a)]. Logical states $|0\rangle_\alpha$ and $|1\rangle_\alpha$ are encoded in long-lived ground or metastable states of the atoms. The atoms are simultaneously irradiated by two global fields with complex Rabi frequency $|\Omega_j(t)|e^{i\phi_j(t)}$, driving the transition $|j\rangle_\alpha \leftrightarrow |r_j\rangle_\alpha$ $(j = 0, 1)$, with $|r_0\rangle_\alpha$ and $|r_1\rangle_\alpha$ two Rydberg states. A detailed discussion on the implementation of the $|j\rangle_\alpha \leftrightarrow |r_j\rangle_\alpha$ transition, including multiphoton processes, is presented in the Supplemental Material [32]. The Rydberg states of the two atoms are coupled by the dipolar spin-exchange interaction J, resulting in the following Hamiltonian in the rotating frame:

$$H(t) = \sum_{j,\alpha} \frac{|\Omega_j(t)|}{2}(e^{i\phi_j(t)}|j\rangle\langle r_j|_\alpha + \text{H.c.}) + J(|r_0r_1\rangle\langle r_1r_0| + \text{H.c.}), \quad (1)$$

with $|r_0r_1\rangle \equiv |r_0\rangle_A \otimes |r_1\rangle_B$ and $\hbar = 1$. Equation (1) neglects spontaneous emission, atomic motion, photon recoil, and residual vdW interactions; their impact and mitigation are discussed below. In principle, Eq. (1) enables an ISWAP gate, $U_{\mathrm{ISWAP}} = |00\rangle\langle 00| + |11\rangle\langle 11| + i(|01\rangle\langle 10| + |10\rangle\langle 01|)$, which, together with single-qubit rotations, forms a universal gate set. The simplest implementation, analogous to schemes with polar molecules [33–38], uses a π pulse to

[*] Contact author: bergonzoni@unistra.fr
[†] Contact author: pupillo@unistra.fr

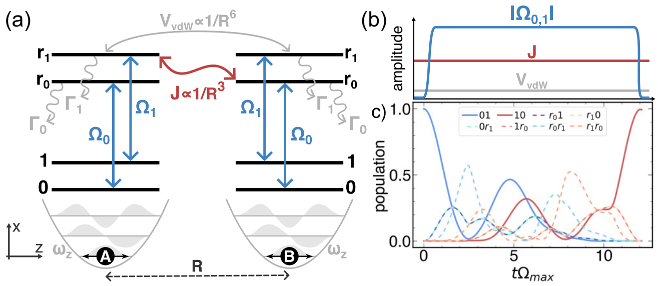

FIG. 1. ISWAP gate with Rydberg atoms. (a) Two atoms separated by a distance R, irradiated by two laser fields $\Omega_{0,1}$, with a resonant dipolar coupling J. Rydberg decay $\Gamma_{0,1}$, atomic motion, and vdW interactions $V_{\rm vdW}$ are also included. (b) A single optimal laser pulse $\Omega_{0,1}$ is applied, with dipolar and vdW interactions present from the outset. (c) Evolution of the two-atom state populations during the pulse for $\Omega_{\rm max}/J = 2.1$ [Fig. 2(c)], starting from the state $|01\rangle$.

excite the atoms to Rydberg states, free evolution under J to generate entanglement, and a second π pulse for deexcitation (see the Supplemental Material [32]). However, in Rydberg systems the dipolar interaction is typically comparable to or larger than the Rabi frequency ($J \gtrsim |\Omega_{0,1}|$), perturbing the π-pulse dynamics. Thus, we propose a protocol where a single continuous laser pulse whose amplitude and—crucially—phase are time dependent and designed via quantum optimal control methods to be time optimal and robust with respect to these interactions during excitation and deexcitation, as well as vdW interactions in the excited states and Rydberg-state spontaneous emission. This enables high-fidelity gates compatible with most quantum error correction schemes over tens of micrometers in the presence of all relevant noise sources, including laser photon recoil, atomic motion, and scattering from intermediate states in multiphoton transitions. Similarly to Rydberg blockade gates [8,39], the continuous global pulse irradiating both atoms is expected to simplify experiments.

As an example, we consider ^{87}Rb, where qubit states can be encoded in the hyperfine levels $|0\rangle_\alpha \equiv |F=1, m_F=0\rangle_\alpha$ and $|1\rangle_\alpha \equiv |F=2, m_F=0\rangle_\alpha$ of the ground-state manifold $5S_{1/2}$, with F the total angular momentum and m_F its projection along the quantization (interatomic) axis z. The Rydberg states $n{\rm S}_{1/2}$ with $m_j = 1/2$ and $n{\rm P}_{3/2}$ with $m_j = 3/2$ are chosen as $|r_0\rangle_\alpha$ and $|r_1\rangle_\alpha$, respectively, with n the principal quantum number. This results in dipolar interaction energies J in the range $0.1\,{\rm GHz} \lesssim J/2\pi \lesssim 1\,{\rm GHz}$, for the considered quantum numbers $n \gtrsim 50$ and interatomic distances $R \sim$ 3–30 µm. We consider realistic Rabi frequencies $1\,{\rm MHz} \leqslant |\Omega_{0,1}|/2\pi \leqslant 10\,{\rm MHz}$.

II. TIME-OPTIMAL GATE

As a first step, we demonstrate a time-optimal scheme for implementing $U_{\rm iSWAP}$ with Eq. (1), i.e., including only the combined effects of J and the laser drive. Time optimality minimizes spontaneous emission, a fundamental error source for Rydberg atoms [3–6,8,11]. As in Rydberg blockade schemes [8,40,41], we define a cost function $1-F$, with F the Bell state fidelity

$$F = \frac{1}{16}\left|\sum_q \langle\psi_q|R^{\otimes 2}U_{\rm iSWAP}|q\rangle\right|^2, \tag{2}$$

where $|\psi_q\rangle$ is the actual two-qubit final state obtained by applying the pulse to $|q\rangle$, from the computational basis $|q\rangle \in \{|00\rangle, |01\rangle, |10\rangle, |11\rangle\}$. $|\psi_q\rangle$ is therefore compared to the target state $U_{\rm iSWAP}|q\rangle$ up to a final global single-qubit operation $R(\theta,\varphi,\lambda) = e^{i(\varphi+\lambda)/2}R_z(\varphi)R_y(\theta)R_z(\lambda)$, where φ, θ, and λ are rotation angles treated as additional optimization parameters. The cost function is numerically minimized using quantum optimal control methods—here, we use the GRAPE algorithm [8,42]. The time-optimal pulse is defined as the shortest pulse that achieves zero infidelity $1-F$, within numerical precision, once a specific Hamiltonian—encoding all the relevant physical interactions and control fields—is fixed. We apply this approach to a wide range of experimentally relevant ratios $0 \lesssim |\Omega_{0,1}|/J \lesssim 10$.

Our first key result is that, for $0 \lesssim |\Omega_{0,1}|/J \lesssim 10$, time-optimal pulses are those for which the amplitudes of the two Rabi frequencies are equal to the maximum available Rabi frequency in experiments, which here we assume identical for the two lasers, i.e., $|\Omega_0(t)| = |\Omega_1(t)| = \Omega_{\rm max}$. In addition, we find that time optimality also requires same lasers phases, i.e., $\phi_0(t) = \phi_1(t) = \phi(t)$, with $\phi(t)$ the key variable to be varied in time to minimize $1-F$, which has not been done before. Figure 2(a) shows an example result of the infidelity $1-F$ versus the total gate duration T for a given ratio

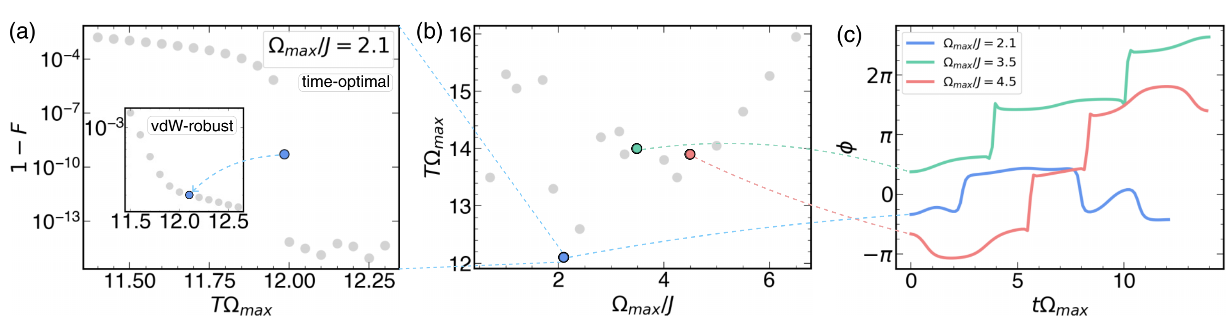

FIG. 2. Time-optimal and vdW-robust (vdW-R) pulses. (a) Minimum infidelity $1-F$ found by GRAPE for pulses of duration T, in units of the Rabi frequency $\Omega_{\rm max}$, for the ratio $\Omega_{\rm max}/J = 2.1$. The time-optimal pulse has duration $T\Omega_{\rm max} = 11.95$; while trying to make it robust to vdW interactions, the pulse durations is increased to $T\Omega_{\rm max} = 12.1$ (inset). (b) Optimal duration T in units of $\Omega_{\rm max}$ vs coupling ratio $\Omega_{\rm max}/J$ of the vdW-robust pulses. The range R and fidelity F obtained for a realistic choice of experimental parameters are shown in Fig. 3. (c) Optimal phase profile $\phi(t)$ of three vdW-robust pulses.

TABLE I. Error budget of the TO and vdW-R pulses for $\Omega_{\max}/J = 2.1$. Reported are infidelities $1-F$ in the presence of individual perturbations: realistic atomic transitions (off-resonant couplings and intermediate state scattering), vdW interactions, Rydberg decay, atomic motion along the interatomic z axis, and photon recoil—considering both its effects: detuning (compensated and uncompensated) and coupling between internal and motional states (for laser orientations along x and z). Experimental parameters used in the simulations: Rabi frequency $\Omega_{\max}/2\pi = 10$ MHz, principal quantum number $n = 100$ of ^{87}Rb, trapping frequencies $\omega_z/2\pi = 100$ kHz, $\omega_x = \omega_z/5$, and temperature $T_{\text{temp}} = 1\,\mu$K.

Noise term		Atomic transitions	vdW H_{vdW}	Decay H_Γ	$z$motion $H_J^{(1,z)} + H_{\text{vdW}}^{(1,z)}$	Recoil (detuning) $\Delta_j = 0$	Recoil (detuning) $\Delta_j = -\frac{2\pi^2}{m\lambda_j^2}$	Recoil (coupling) $\bar{\ell} = x$	Recoil (coupling) $\bar{\ell} = z$	All
$1-F$	TO	5.5×10^{-3}	1.3×10^{-2}	7.0×10^{-4}	4.3×10^{-5}	1.3×10^{-5}	$<10^{-7}$	2.3×10^{-5}	4.9×10^{-5}	1.9×10^{-2}
	vdW-R	4.1×10^{-3}	2.0×10^{-4}	7.0×10^{-4}	3.7×10^{-5}	8.7×10^{-6}	$<10^{-7}$	1.9×10^{-5}	5.1×10^{-5}	5.1×10^{-3}

$\Omega_{\max}/J = 2.1$, with T in units of $\Omega_{\max}$. The figure shows that the infidelity decreases abruptly to numerical zero around $T\Omega_{\max} = 11.95$ (blue dot), corresponding to the time-optimal pulse. Varying the ratio $\Omega_{\max}/J$ results in different optimal phase profiles and gate durations, with the shortest pulse obtained for $\Omega_{\max}/J = 0.7$, corresponding to $T\Omega_{\max} = 8.2$. This is essentially the same timescale of the time-optimal blockade gate ($T\Omega_{\max} = 7.5$) [8] or the recently proposed short-range resonant dipole-dipole cz gate ($T\Omega_{\max} = 5.95$) [28]. However, here the range of the gate scales as $R \sim \sqrt[3]{n^4(\Omega_{\max}/J)/\Omega_{\max}}$, which allows to reach distances of tens of micrometers. For example, for $\Omega_{\max}/2\pi = 10\,(5)$ MHz, $\Omega_{\max}/J = 2.1\,(4.25)$, and $n = 100$, we obtain $R = 20\,(31)\,\mu$m. We find that the optimal T versus $\Omega_{\max}/J$ is not monotonic (see the Supplemental Material [32]), but generally increases with $\Omega_{\max}/J$. While shorter pulses would minimize spontaneous emission, they are more susceptible to atomic motion and vdW interactions, and therefore do not necessarily yield the optimal solution in realistic scenarios, which we address next.

III. IMPERFECTIONS AND ROBUSTNESS

The relevant Hamiltonian to realize U_{iSWAP} gates with neutral atoms beyond Eq. (1) reads $H' = H'_\Omega + H'_J + H'_{\text{vdW}} + H_K + H_\Gamma$, with

$$H'_\Omega = \sum_{j,\alpha} \frac{\Omega_j}{2}[e^{i\phi_j + i\eta_j(a_{\bar{\ell},\alpha} + a_{\bar{\ell},\alpha}{}^\dagger)}|j\rangle\langle r_j|_\alpha + \text{H.c.}],$$

$$H'_J = J\left[1 - 3\frac{z_A - z_B}{R}\right](|r_0 r_1\rangle\langle r_1 r_0| + \text{H.c.}),$$

$$H'_{\text{vdW}} = \sum_{i,j} V_{ij}\left[1 - 6\frac{z_A - z_B}{R}\right]|r_i r_j\rangle\langle r_i r_j|,$$

$$H_K = -\sum_{\alpha,\ell}\frac{p^2_{\alpha,\ell}}{2m}, \quad H_\Gamma = -\frac{i}{2}\sum_{j,\alpha}\Gamma_j|r_j\rangle\langle r_j|_\alpha. \qquad (3)$$

The term H'_Ω in Eq. (3) includes the effect of photon recoil in the laser driving Hamiltonian, characterized by the Lamb-Dicke parameter η_j, and with $a_{\bar{\ell},\alpha}{}^\dagger$ and $a_{\bar{\ell},\alpha}$ the ladder operators for the harmonic trap of atom α along the laser propagation direction $\bar{\ell}$ [28,43]. The term H'_J includes the first-order correction in the dipole-dipole interaction J of Eq. (1), arising from atomic motion along the interatomic direction z, where z_α is the position operator of atom α in its radial harmonic trap (see the Supplemental Material [32]). H'_{vdW} describes off-resonant van der Waals interactions and their first-order position-dependent corrections $H^{(1,z)}_{\text{vdW}}$ in the z direction. H_K is the kinetic operator, with m the atomic mass and $p_{\alpha,\ell}$ the momentum operator of atom α along the three axis $\ell = x, y, z$. The trapping potential is here omitted as optical tweezers are usually turned off during the Rydberg excitation pulses [3,44]. Finally, H_Γ in Eq. (3) is a non-Hermitian term describing decay from Rydberg states with rates $\Gamma_{0,1}$.

Photon recoil has a twofold effect: First, it introduces a constant detuning $\Delta_j = 2\pi^2/(m\lambda_j^2)$ corresponding to the kinetic energy imparted by a photon of laser j, with wavelength λ_j. Second, it induces a coupling between motional degrees of freedom along the $\bar{\ell}$ direction and the internal states of the atom, with strength $\sim\sqrt{\omega_{\bar{\ell}}/(m\lambda_j^2)}$ and with $\omega_{\bar{\ell}}$ the trapping frequency in the laser direction (see the Supplemental Material [32]). This results in decoherence of the internal states by entanglement of motional and electronic states. H'_J results in further coupling between motional degrees of freedom and internal states of the atom—with coupling strength $\sim J/(R\sqrt{m\omega_z})$—due to quantum mechanical motional spread of the wave functions. Similar effects are observed for van der Waals interactions H_{vdW}. Table I provides an example of error budget resulting from the terms in Eq. (3) for the time-optimal pulse with $\Omega_{\max}/J = 2.1$, for a choice of realistic experimental parameters. The table shows that vdW interactions largely dominate the error budget, accounting for an infidelity $1 - F \sim 10^{-2}$, while all other error sources provide orders of magnitude smaller contributions (see the Supplemental Material [32] for details).

In this work, we therefore proceed to obtain higher-fidelity gates by making the TO pulses robust against vdW interactions. This is achieved by including the latter directly in the optimization, using the TO pulses as initial guess [28]. In general, for small ratios $\Omega_{\max}/J \lesssim 1$—corresponding to smaller interatomic distances R—the numerical optimization fails to find a robust pulse with a duration T comparable to the TO one. For larger ratios $\Omega_{\max}/J \gtrsim 3$, however, we find pulses with high fidelity while maintaining almost the same pulse duration, as a result of the short-range nature of vdW interactions. Figure 2(b) shows the minimum vdW-robust gate duration T as a function of $\Omega_{\max}/J$: For $\Omega_{\max}/J = 2.1$, the robust pulse duration is $T\Omega_{\max} = 12.1$. This is less than 2% longer than the corresponding TO pulse [see Fig. 2(a)], but with infidelity well below 10^{-3} in the presence of vdW

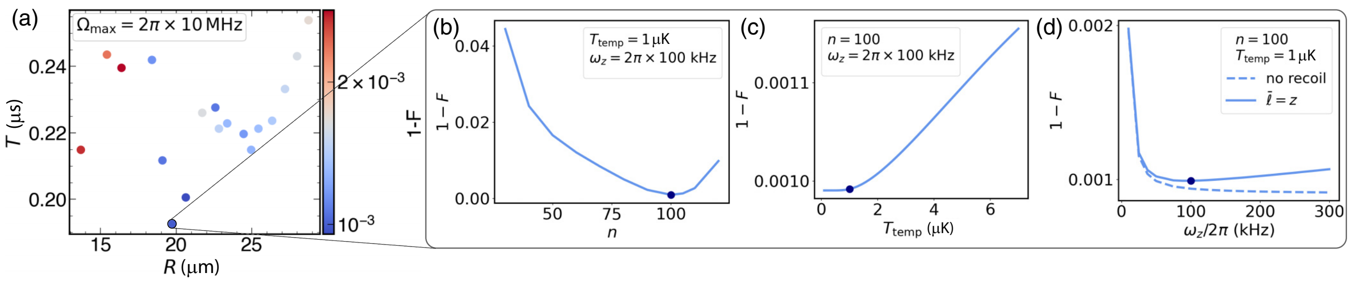

FIG. 3. Infidelity of the vdW-robust pulses for a fixed Rabi frequency $\Omega_{max}/2\pi = 10$ MHz—without accounting for the errors from realistic atomic transitions. (a) Heat map of gate infidelity $1 - F$ (color scale on the right) for several coupling ratios Ω_{max}/J, with $1.5 \leqslant J \leqslant 15$ MHz. Fidelity of the vdW-robust pulse for $\Omega_{max}/J = 2.1$ as a function of (b) the principal quantum number n, (c) the atomic temperature T_{temp}, and (d) the radial trapping frequency $\omega_z/2\pi$, in absence of photon recoil and with the laser orientated along the interatomic direction ($\bar{\ell} = z$).

interactions only. Increasing the duration T of the robust pulse can further decrease the infidelity [see inset in Fig. 2(a)]. Figure 2(c) plots the optimal phase $\phi(t)$ for three representative pulses: In all cases, the pulses are smooth in time, which should make them easier to implement in experiments. Jumps of π in the phase for $\Omega_{max}/J > 2.1$ can in principle be removed by reoptimizing the pulse for the detuning—instead of the phase only—and fixing a cutoff, with minimal loss of pulse performance [45].

Figure 3(a) analyzes of a set of vdW-robust pulses for different values of the ratio Ω_{max}/J, including all terms in Eq. (3). The pulse with $\Omega_{max}/J = 2.1$—assuming a Rabi frequency $\Omega_{max}/2\pi = 10\,(5)$ MHz, radial trapping frequency $\omega_z/2\pi = 100$ kHz, temperature $T_{temp} = 1\,\mu$K, and principal quantum number $n = 100$ of ^{87}Rb—yields an infidelity $1 - F < 1\,(3) \times 10^{-3}$, at an interatomic distance $R = 20\,(31)\,\mu$m with total pulse duration $T = 197\,(430)$ ns. This is comparable to that of cz gates based on the blockade mechanism [3,4,8]. To cover the same distance, the state-of-the-art qubit transport would require times that are three orders of magnitude longer [16]. The fidelity in Fig. 3(a) remains high, $1 - F \leqslant 2 \times 10^{-3}$, even for larger ratios $\Omega_{max}/J \lesssim 7$, allowing the implementation of entangling pulses between even more distant atoms, $R \approx 30\,\mu$m, on submicrosecond timescales.

In Figs. 3(b)–3(d), the fidelity of the robust pulse $\Omega_{max}/J = 2.1$ is analyzed as a function of the principal quantum number n, the temperature T_{temp}, and the radial trapping frequency ω_z. Increasing n shortens the pulse duration, since $J \sim n^4$, and increases the Rydberg lifetime $\Gamma \sim n^{-3}$, thus reducing infidelity, provided the pulse remains robust against the corresponding vdW interactions; otherwise, larger n amplifies their perturbative effect $V_{vdW} \sim n^{11}$ [see Fig. 3(b)]. This improvement is partially offset by the decrease of the Rabi frequency $\Omega_{max} \sim n^{-3/2}$ [1]. Lower temperatures reduce the occupation of excited motional states and hence position uncertainty [see Fig. 3(c)]. The trapping frequency also plays a crucial role: The displacement operator scales as $1/\sqrt{\omega_z}$, whereas the momentum kick grows as $\sqrt{\omega_{\bar{\ell}}}$. If lasers are aligned along the interatomic direction $\bar{\ell} = z$, a trade-off between position fluctuations and photon recoil leads to an optimal confinement near $\omega_z^* \approx 90$ kHz [solid line in Fig. 3(d)], as documented in Refs. [27,28,40,43]. If the lasers are along the more weakly confined axial direction $\bar{\ell} = x$, with typically $\omega_z \approx 5\omega_x$, photon recoil effects are suppressed and the optimal confinement becomes much larger [dashed line in Fig. 3(d)].

In addition to the error sources in Eq. (3), one must account for errors from realistic atomic transitions (see the Supplemental Material [32]), in particular, scattering from the intermediate state $|e\rangle = |6P_{3/2}, F = 2, m_F = 1\rangle$ in the two-photon excitation to $|r_0\rangle$, as well as off-resonant couplings to other Rydberg states, such as $|r_0'\rangle = |98D_{5/2}, m_j = -3/2\rangle$ and $|r_1'\rangle = |100P_{3/2}, m_j = 1/2\rangle$, that induce unwanted Stark shifts and population leakage. These effects increase the infidelity up to $1 - F \approx 5.1\,(8.4) \times 10^{-3}$ for $\Omega_{max}/J = 2.1\,(4.25)$ and $\Omega_{max} = 10\,(5)$ MHz, with an intermediate detuning $\Delta_e = 40\,\Omega_{max}$ and a magnetic field $B = 50\,(20)$ G. The resulting fidelities remain compatible with most quantum error-correction schemes.

IV. CONCLUSION

We have demonstrated a protocol for time-optimal, high-fidelity ISWAP gates between neutral atoms separated by tens of micrometers. The scheme combines resonant dipolar spin-exchange interactions with optimally shaped laser pulses, achieving gate speeds comparable to the fastest cz gates at few-micrometer distances. The fidelities reached are compatible with error-correction thresholds [46], with further improvements possible by mitigating residual errors listed in Table I. In particular, recoil-induced detuning can be corrected via laser frequency fine-tuning, and motional-electronic coupling reduced by aligning beams along the weakly confined axial direction. Using heavier species, such as ^{133}Cs, further suppresses motional errors. These results open several directions. The approach can be extended to k-qubit gates ($k > 2$) via resonant dipole-dipole interactions, enhancing stabilizer efficiency [47,48] while reducing gate count and circuit depth [49]. Fast, long-range gates enable efficient quantum information transport across neutral-atom registers without intermediate operations, ancillary qubits, or atomic motion—crucial for modular quantum computing and error correction. Moreover, these gates can facilitate recently developed low-density parity-check codes, which require stabilizer qubits separated by large distances [48,50–53]. Exploiting long-range interactions, such codes achieve higher encoding rates, reduced qubit overhead, and larger code distances d, yielding lower logical error probabilities than surface codes of comparable size.

See the Supplemental Material [32] for details on the optimization algorithm, physical implementation, and fidelity.

ACKNOWLEDGMENTS

We are grateful to S. Whitlock for insightful discussions. This research has received funding from the European Union's Horizon Europe program Grant No. HORIZON-CL4-2021-DIGITAL-EMERGING-01-30 via the Project No. 101070144 (EuRyQa) and from the French National Research Agency under the Investments of the Future Program Projects No. ANR-21-ESRE-0032 (aQCess), ANR-22-CE47-0013-02 (CLIMAQS), and ANR-22-CMAS-0001 France 2030 (QuanTEdu-France) and support from the Institut Universitaire de France (IUF).

DATA AVAILABILITY

The data that support the findings of this article are openly available [67].

[1] M. Saffman, T. G. Walker, and K. Mølmer, Quantum information with Rydberg atoms, Rev. Mod. Phys. **82**, 2313 (2010).

[2] M. Morgado and S. Whitlock, Quantum simulation and computing with Rydberg-interacting qubits, AVS Quantum Sci. **3**, 023501 (2021).

[3] S. J. Evered, D. Bluvstein, M. Kalinowski, S. Ebadi, T. Manovitz, H. Zhou, S. H. Li, A. A. Geim, T. T. Wang, N. Maskara, H. Levine, G. Semeghini, M. Greiner, V. Vuletić, and M. D. Lukin, High-fidelity parallel entangling gates on a neutral-atom quantum computer, Nature (London) **622**, 268 (2023).

[4] S. Ma, G. Liu, P. Peng, B. Zhang, S. Jandura, J. Claes, A. P. Burgers, G. Pupillo, S. Puri, and J. D. Thompson, High-fidelity gates and mid-circuit erasure conversion in an atomic qubit, Nature (London) **622**, 279 (2023).

[5] R. B.-S. Tsai, X. Sun, A. L. Shaw, R. Finkelstein, and M. Endres, Benchmarking and fidelity response theory of high-fidelity Rydberg entangling gates, PRX Quantum **6**, 010331 (2025).

[6] J. A. Muniz, M. Stone, D. T. Stack, M. Jaffe, J. M. Kindem, L. Wadleigh, E. Zalys-Geller, X. Zhang, C.-A. Chen, M. A. Norcia, *et al.*, High-fidelity universal gates in the ^{171}Yb ground-state nuclear-spin qubit, PRX Quantum **6**, 020334 (2025).

[7] D. Jaksch, J. I. Cirac, P. Zoller, S. L. Rolston, R. Côté, and M. D. Lukin, Fast quantum gates for neutral atoms, Phys. Rev. Lett. **85**, 2208 (2000).

[8] S. Jandura and G. Pupillo, Time-optimal two- and three-qubit gates for Rydberg atoms, Quantum **6**, 712 (2022).

[9] H. Levine, A. Keesling, G. Semeghini, A. Omran, T. T. Wang, S. Ebadi, H. Bernien, M. Greiner, V. Vuletić, H. Pichler, and M. D. Lukin, Parallel implementation of high-fidelity multiqubit gates with neutral atoms, Phys. Rev. Lett. **123**, 170503 (2019).

[10] A. Radnaev, W. Chung, D. Cole, D. Mason, T. Ballance, M. Bedalov, D. Belknap, M. Berman, M. Blakely, I. Bloomfield *et al.*, Universal neutral-atom quantum computer with individual optical addressing and nondestructive readout, PRX Quantum **6**, 030334 (2025).

[11] M. Peper, Y. Li, D. Y. Knapp, M. Bileska, S. Ma, G. Liu, P. Peng, B. Zhang, S. P. Horvath, A. P. Burgers, and J. D. Thompson, Spectroscopy and modeling of ^{171}Yb Rydberg states for high-fidelity two-qubit gates, Phys. Rev. X **15**, 011009 (2025).

[12] J.-L. Wu, Y. Wang, J.-X. Han, Y.-K. Feng, S.-L. Su, Y. Xia, Y. Jiang, and J. Song, One-step implementation of Rydberg-antiblockade SWAP and controlled-SWAP gates with modified robustness, Photon. Res. **9**, 814 (2021).

[13] J.-L. Wu, Y. Wang, J.-X. Han, S.-L. Su, Y. Xia, Y. Jiang, and J. Song, Unselective ground-state blockade of Rydberg atoms for implementing quantum gates, Front. Phys. **17**, 22501 (2022).

[14] W.-X. Li, J.-L. Wu, S.-L. Su, and J. Qian, High-tolerance antiblockade swap gates using optimal pulse drivings, Phys. Rev. A **109**, 012608 (2024).

[15] S.-L. Su and W. Li, Dipole-dipole-interaction–driven antiblockade of two Rydberg atoms, Phys. Rev. A **104**, 033716 (2021).

[16] M. Saffman, Quantum computing with atomic qubit arrays: Confronting the cost of connectivity, arXiv:2505.11218.

[17] G. Pichard, D. Lim, E. Bloch, J. Vaneecloo, L. Bourachot, G.-J. Both, G. Mériaux, S. Dutartre, R. Hostein, J. Paris, B. Ximenez, A. Signoles, A. Browaeys, T. Lahaye, and D. Dreon, Rearrangement of individual atoms in a 2000-site optical-tweezer array at cryogenic temperatures, Phys. Rev. Appl. **22**, 024073 (2024).

[18] H. Zhou, C. Zhao, M. Cain, D. Bluvstein, N. Maskara, C. Duckering, H.-Y. Hu, S.-T. Wang, A. Kubica, and M. D. Lukin, Low-overhead transversal fault tolerance for universal quantum computation, Nature (London) **646**, 303 (2025).

[19] I. N. Ashkarin, S. Lepoutre, P. Pillet, I. I. Beterov, I. I. Ryabtsev, and P. Cheinet, Long-range $CC\Phi$ gates via radio-frequency-induced Förster resonances, Phys. Rev. Res. **7**, 013034 (2025).

[20] D. Kurdak, P. R. Banner, Y. Li, S. R. Muleady, A. V. Gorshkov, S. L. Rolston, and J. V. Porto, Enhancement of Rydberg blockade via microwave dressing, Phys. Rev. Lett. **134**, 123404 (2025).

[21] A. Cesa and J. Martin, Two-qubit entangling gates between distant atomic qubits in a lattice, Phys. Rev. A **95**, 052330 (2017).

[22] Y. Sun, Buffer-atom-mediated quantum logic gates with off-resonant modulated driving, Sci. China: Phys. Mech. Astron. **67**, 120311 (2024).

[23] G. Doultsinos and D. Petrosyan, Quantum gates between distant atoms mediated by a Rydberg excitation antiferromagnet, Phys. Rev. Res. **7**, 023246 (2025).

[24] A. Reinhard, T. C. Liebisch, B. Knuffman, and G. Raithel, Level shifts of rubidium Rydberg states due to binary interactions, Phys. Rev. A **75**, 032712 (2007).

[25] Y. Chew, T. Tomita, T. P. Mahesh, S. Sugawa, S. de Léséleuc, and K. Ohmori, Ultrafast energy exchange between two single Rydberg atoms on a nanosecond timescale, Nat. Photon. **16**, 724 (2022).

[26] P. Méhaignerie, Y. Machu, A. Durán Hernández, G. Creutzer, D. J. Papoular, J. M. Raimond, C. Sayrin, and M. Brune, Interacting circular Rydberg atoms trapped in optical tweezers, PRX Quantum **6**, 010353 (2025).

[27] G. Emperauger, M. Qiao, G. Bornet, C. Chen, R. Martin, Y. T. Chew, B. Gély, L. Klein, D. Barredo, A. Browaeys, and T. Lahaye, Benchmarking direct and indirect dipolar spin-exchange interactions between two Rydberg atoms, Phys. Rev. A **111**, 062806 (2025).

[28] G. Giudici, S. Veroni, G. Giudice, H. Pichler, and J. Zeiher, Fast entangling gates for Rydberg atoms via resonant dipole-dipole interaction, PRX Quantum **6**, 030308 (2025).

[29] J. T. Young, P. Bienias, R. Belyansky, A. M. Kaufman, and A. V. Gorshkov, Asymmetric blockade and multiqubit gates via dipole-dipole interactions, Phys. Rev. Lett. **127**, 120501 (2021).

[30] E. Crane, A. Schuckert, N. H. Le, and A. J. Fisher, Rydberg entangling gates in silicon, Phys. Rev. Res. **3**, 033086 (2021).

[31] P. Ildefonso, A. Byun, A. Konovalov, J. Kazemi, M. Schuler, and W. Lechner, Expanding the neutral atom gate set: Native iswap and exchange gates from dipolar Rydberg interactions, arXiv:2512.05037.

[32] See Supplemental Material at https://link.aps.org/supplemental/10.1103/hjrh-4327 for details on the optimization algorithm, physical implementation, and fidelity, which also include Refs. [54–67].

[33] K.-K. Ni, T. Rosenband, and D. D. Grimes, Dipolar exchange quantum logic gate with polar molecules, Chem. Sci. **9**, 6830 (2018).

[34] C. M. Holland, Y. Lu, and L. W. Cheuk, On-demand entanglement of molecules in a reconfigurable optical tweezer array, Science **382**, 1143 (2023).

[35] Y. Bao, S. S. Yu, L. Anderegg, E. Chae, W. Ketterle, K.-K. Ni, and J. M. Doyle, Dipolar spin-exchange and entanglement between molecules in an optical tweezer array, Science **382**, 1138 (2023).

[36] L. R. B. Picard, A. J. Park, G. E. Patenotte, S. Gebretsadkan, D. Wellnitz, A. M. Rey, and K.-K. Ni, Entanglement and iSWAP gate between molecular qubits, Nature (London) **637**, 821 (2025).

[37] D. K. Ruttley, T. R. Hepworth, A. Guttridge, and S. L. Cornish, Long-lived entanglement of molecules in magic-wavelength optical tweezers, Nature (London) **637**, 827 (2025).

[38] M. Bergonzoni, S. Jandura, and G. Pupillo, iSWAP gate with polar molecules: Robustness criteria for entangling operations, Phys. Rev. A **112**, 032621 (2025).

[39] D. Bluvstein, S. J. Evered, A. A. Geim, S. H. Li, H. Zhou, T. Manovitz, S. Ebadi, M. Cain, M. Kalinowski, D. Hangleiter, *et al.*, Logical quantum processor based on reconfigurable atom arrays, Nature (London) **626**, 58 (2024).

[40] A. Pagano, S. Weber, D. Jaschke, T. Pfau, F. Meinert, S. Montangero, and H. P. Büchler, Error budgeting for a controlled-phase gate with strontium-88 Rydberg atoms, Phys. Rev. Res. **4**, 033019 (2022).

[41] M. Mohan, R. de Keijzer, and S. Kokkelmans, Robust control and optimal Rydberg states for neutral atom two-qubit gates, Phys. Rev. Res. **5**, 033052 (2023).

[42] N. Khaneja, T. Reiss, C. Kehlet, T. Schulte-Herbrüggen, and S. J. Glaser, Optimal control of coupled spin dynamics: Design of NMR pulse sequences by gradient ascent algorithms, J. Magn. Reson. **172**, 296 (2005).

[43] F. Robicheaux, T. M. Graham, and M. Saffman, Photon-recoil and laser-focusing limits to Rydberg gate fidelity, Phys. Rev. A **103**, 022424 (2021).

[44] Z. Zuo, M. Fukusen, Y. Tamaki, T. Watanabe, Y. Nakagawa, and K. Nakagawa, Single atom Rydberg excitation in a small dipole trap, Opt. Express **17**, 22898 (2009).

[45] L. Pecorari, S. Jandura, and G. Pupillo, Low-depth quantum error correction via three-qubit gates in Rydberg atom arrays, Phys. Rev. Lett. **135**, 240602 (2025).

[46] A. G. Fowler, M. Mariantoni, J. M. Martinis, and A. N. Cleland, Surface codes: Towards practical large-scale quantum computation, Phys. Rev. A **86**, 032324 (2012).

[47] J. Old, S. Tasler, M. J. Hartmann, and M. Müller, Fault-tolerant stabilizer measurements in surface codes with three-qubit gates, Phys. Rev. Lett. **135**, 240601 (2025).

[48] L. Pecorari, S. Jandura, G. K. Brennen, and G. Pupillo, High-rate quantum LDPC codes for long-range-connected neutral atom registers, Nat. Commun. **16**, 1111 (2025).

[49] J. M. Baker, A. Litteken, C. Duckering, H. Hoffmann, H. Bernien, and F. T. Chong, Exploiting long-distance interactions and tolerating atom loss in neutral atom quantum architectures, in *Proceedings of the 48th Annual International Symposium on Computer Architecture (ISCA '21), Virtual Event, Spain* (IEEE Press, 2021), pp. 818–831.

[50] M. A. Tremblay, N. Delfosse, and M. E. Beverland, Constant-overhead quantum error correction with thin planar connectivity, Phys. Rev. Lett. **129**, 050504 (2022).

[51] S. Bravyi, A. W. Cross, J. M. Gambetta, D. Maslov, P. Rall, and T. J. Yoder, High-threshold and low-overhead fault-tolerant quantum memory, Nature (London) **627**, 778 (2024).

[52] Q. Xu, J. P. Bonilla Ataides, C. A. Pattison, N. Raveendran, D. Bluvstein, J. Wurtz, B. Vasić, M. D. Lukin, L. Jiang, and H. Zhou, Constant-overhead fault-tolerant quantum computation with reconfigurable atom arrays, Nat. Phys. **20**, 1084 (2024).

[53] C. Poole, T. M. Graham, M. A. Perlin, M. Otten, and M. Saffman, Architecture for fast implementation of quantum low-density parity-check codes with optimized Rydberg gates, Phys. Rev. A **111**, 022433 (2025).

[54] A. Uhlmann, The "transition probability" in the state space of a *-algebra, Rep. Math. Phys. **9**, 273 (1976).

[55] N. Šibalić, J. Pritchard, C. Adams, and K. Weatherill, Arc: An open-source library for calculating properties of alkali Rydberg atoms, Comput. Phys. Commun. **220**, 319 (2017).

[56] L. Chomaz, I. Ferrier-Barbut, F. Ferlaino, B. Laburthe-Tolra, B. L. Lev, and T. Pfau, Dipolar physics: A review of experiments with magnetic quantum gases, Rep. Prog. Phys. **86**, 026401 (2023).

[57] M. L. Wall, K. Maeda, and L. D. Carr, Realizing unconventional quantum magnetism with symmetric top molecules, New J. Phys. **17**, 025001 (2015).

[58] P. Virtanen, R. Gommers, T. E. Oliphant, M. Haberland, T. Reddy, D. Cournapeau, E. Burovski, P. Peterson, W. Weckesser, J. Bright, *et al.*, SciPy 1.0: Fundamental algorithms for scientific computing in Python, Nat. Methods **17**, 261 (2020).

[59] R. J. P. T. de Keijzer, O. Tse, and S. J. J. M. F. Kokkelmans, Recapture probability for antitrapped Rydberg states in optical tweezers, Phys. Rev. A **108**, 023122 (2023).

[60] M. A. Nielsen and I. L. Chuang, *Quantum Computation and Quantum Information* (Cambridge University Press, Cambridge, UK, 2010).

[61] K.-J. Boller, A. Imamoğlu, and S. E. Harris, Observation of electromagnetically induced transparency, Phys. Rev. Lett. **66**, 2593 (1991).

[62] D. Møller, L. B. Madsen, and K. Mølmer, Quantum gates and multiparticle entanglement by Rydberg excitation blockade and adiabatic passage, Phys. Rev. Lett. **100**, 170504 (2008).

[63] A. M. Hankin, Y.-Y. Jau, L. P. Parazzoli, C. W. Chou, D. J. Armstrong, A. J. Landahl, and G. W. Biedermann, Two-atom Rydberg blockade using direct 6*s* to *np* excitation, Phys. Rev. A **89**, 033416 (2014).

[64] B. Li, M. Li, X. Jiang, J. Qian, X. Li, L. Liu, and Y. Wang, Optical spectroscopy of *np* Rydberg states of ^{87}Rb atoms with a 297-nm ultraviolet laser, Phys. Rev. A **99**, 042502 (2019).

[65] M. Saffman, Quantum computing with atomic qubits and Rydberg interactions: Progress and challenges, J. Phys. B: At. Mol. Opt. Phys. **49**, 202001 (2016).

[66] Y.-Y. Jau, A. M. Hankin, T. Keating, I. H. Deutsch, and G. W. Biedermann, Entangling atomic spins with a Rydberg-dressed spin-flip blockade, Nat. Phys. **12**, 71 (2016).

[67] M. Bergonzoni and G. Pupillo, Pulse data for "Fast quantum gates for neutral atoms separated by a few tens of micrometers", figshare data repository (2025), https://doi.org/10.6084/m9.figshare.30739526.